Pergamon

Geochimica et Cosmochimica Acta, Vol. 65, No. 16, pp. 2709–2722, 2001

0016-7037/01 $20.00 + .00

PII S0016-7037(01)00633-0

An X-ray absorption spectroscopy study of the structure and reversibility of copper adsorbed to montmorillonite clay

JOHN D. MORTON,[1] JEREMY D. SEMRAU,[1] and KIM F. HAYES*[1]

[1]Environmental and Water Resources Engineering Program, Department of Civil and Environmental Engineering, University of Michigan, Ann Arbor, MI, USA

(*Received June* 1, 2000; *accepted in revised form March* 27, 2001)

Abstract—X-ray absorption spectroscopy (XAS) and adsorption-desorption measurements have been performed to assess the relationship between the structure and reversibility of copper complexes on montmorillonite clay. By varying the solution pH and background electrolyte concentration, the adsorption of copper on either the edge sites or permanent charge sites of montmorillonite was controlled. This allowed the structure and reversibility of copper complexes on each of these site types to be assessed independently of each other. XAS analysis of copper adsorbed on the permanent charge sites indicated outer-sphere surface complexes, with these complexes showing sorption reversibility. For copper complexes formed on the edge sites of montmorillonite, XAS data confirmed the presence of monomer and dimer copper surface complexes. Sorption irreversibility at edge sites was noted at copper coverages less than 20 μmoles/g clay at pH=4.2 and at coverages greater than 50 μmoles/g clay at pH=6.8. At pH=6.8, higher Cu-Cu coordination numbers indicated the copper sorption irreversibility may be due, in part, to the formation of dimer surface complexes. The coordination numbers at pH=4.2 indicated the irreversibility could be due to the formation of dimers or due to formation of surface complexes on high energy edge sites. *Copyright © 2001 Elsevier Science Ltd*

1. INTRODUCTION

Sorption processes often control the speciation of metal ions in low temperature aqueous geochemical environments (Davis and Kent, 1990; Hayes and Katz, 1995), and thus influence metal mobility, toxicity and bioavailability (McBride, 1994; Hayes and Traina, 1998). Although the importance of sorption processes in sequestering metal ions is well known, the characteristics of the sorption processes that determine the extent of metal ion bioavailability or mobility are largely unknown. In particular, the influence of the structure and composition of adsorbed metal complexes on desorption processes has not been widely addressed in the geochemical literature.

Fe, Mn, and Al oxides, hydroxides, and oxyhydroxides as well as aluminosilicate clay minerals are among the most significant geosorbents for metal ions in subsurface geochemical settings. Spectroscopic studies have identified a variety of types of metal ion complexes that can form on the surface functional groups of these types of metal oxides and clays. These include outer-sphere complexes (Papelis and Hayes, 1996; Chen and Hayes, 1999; Bargar et al., 1996; Strawn et al., 1999), inner-sphere complexes (O'Day et al., 1994a; Schlegel et al., 1999; Strawn and Sparks, 1999), multinuclear complexes and surface precipitates (Chisholm-Brause et al., 1990; O'Day et al., 1994b; Papelis and Hayes, 1996; Bargar et al., 1997a; Chen and Hayes, 1999; Scheidegger et al., 1998; Hudson et al., 1999; Strawn and Sparks, 1999). These complexes differ in the degree of hydration of the adsorbed metal, the number and type of atoms neighboring the adsorbed metal, and the number of surface atoms to which the sorbed species may be attached. With these differences, adsorbed metals are likely to vary in their stability and resistance to desorption. Only a limited number of experimental studies have explored this issue despite the assumed connection between the type of metal ion-surface association and relative metal ion mobility in aqueous geochemical settings.

Some studies have shown that metal ions adsorbed as outer-sphere complexes can be displaced by high concentrations of weakly adsorbing ions such as Na^+ or Ca^{2+} while metals adsorbed as inner-sphere complexes cannot be as easily displaced (Chen and Hayes, 1999; Papelis and Hayes, 1996; Strawn and Sparks, 1999). In addition, several recent studies have attributed differences in desorption behavior to the type of complex or phase formed on clays and oxides (Strawn et al., 1998; Martinez and McBride, 2000; Thompson et al., 2000). In some instances (Strawn et al., 1998; Thompson et al., 2000), inner-sphere complexes, characterized as either monomeric or polymeric, tended to desorb to a greater extent than the precipitate phases found under these experimental conditions. In addition, when surface precipitates were found, the extent of desorption or metal solubility varied depending on the type of precipitate and aging time (Martinez and McBride, 2000; Thompson et al., 2000).

One method to more fully understand the relationship between the structure and composition of metal sorption complexes and desorption behavior, is to systematically study desorption under conditions where the types of sorption complexes formed can be identified and assessed independently. Metals form several types of complexes on smectite clays that are geochemically important and can be assessed independently by varying the experimental conditions of adsorption. Specifically, metals can form complexes on the siloxane ditrigonal cavities of the permanent charge interlayer or on the hydroxyl edge sites where the crystal structure is interrupted. Divalent metal ion adsorption has been distinguished by the effect of solution pH and background electrolyte concen-

* Author to whom correspondence should be addressed (ford@engin.umich.edu).

tration on adsorption on these sites (Papelis and Hayes, 1996; Zachara et al., 1993; Chen and Hayes, 1999; Fletcher and Sposito, 1989; Strawn and Sparks, 1999). With increasing background electrolyte concentration, ions such as Na^+ or Ca^{2+} exchange for copper on the permanent charge sites, causing decreased copper adsorption on these sites. With increasing pH, hydroxyl edge sites on clays deprotonate, increasing copper adsorption on these sites. The relative distribution of divalent metal ions between the two types of adsorption sites can be changed by varying the pH and background electrolyte concentration. Using this information the molecular structure and macroscopic adsorption behavior of metal ions on the permanent charge sites can then be assessed independently of adsorption on the edge sites (Zachara et al., 1993; Chen and Hayes, 1999; Papelis and Hayes, 1996).

To date, a number of spectroscopic investigations have provided insight into the structure of copper complexes formed on clay interlayer sites. These studies indicate that copper adsorbs in the interlayer as an outer-sphere complex (Brown and Kevan, 1988; McBride, 1982; Hyun et al., 2000) and as inner-sphere monomer or multlinuclear complexes on edge (Hyun et al., 2000), steps or kink clay sites (Farquhar et al., 1996). A recent electron paramagnetic resonance (EPR) spectroscopic study performed on copper adsorbed to montmorillonite (Hyun et al. 2000) suggested that copper formed outer-sphere associations in the interlayer at low pH, inner-sphere surface complexes on edge sites at intermediate pH and dimers at higher pH. A number of spectroscopic studies have also been performed using other transition and heavy metals and non-swelling aluminosilicate clays. For example, based on an XAS and extended absorption fine structure analysis (EXAFS) study, Co(II) has been found to form multinuclear complexes under conditions in which sorption to the edge sites of montmorillonite was expected (Papelis and Hayes, 1996; Chen and Hayes, 1999; O'Day et al., 1994a). Using EPR, Clark and McBride (1984) found that copper adsorbed on the edge sites of the aluminosilicates allophane and imogolite as inner-sphere complexes. Furthermore, a recent study by Schlegel et al. (1999) using polarized EXAFS analysis of Co sorbed to self-supporting films of hectorite confirmed the presence of mononuclear inner-sphere Co complexes under pH and surface coverage conditions where multinuclear species formation was intentionally avoided. Based on the results from these systems, copper was expected to form similar associations in the systems selected for this work, i.e., outer-sphere complexes in the interlayer of montmorillonite, and mononuclear and multinuclear complexes at the clay edge, depending on the pH and surface coverage conditions.

Although many studies have characterized the surface associations between metal ions and smectite clays, only a few have assessed reversibility (McClaren et al., 1983; Wu et al., 1999). From a rate and extent of desorption viewpoint, these studies have shown that a fraction of the adsorbed metal ion is reversibly adsorbed and a fraction irreversibly adsorbed. However, these studies were performed under conditions where the types of surface complexes formed were unknown, and thus irreversible and reversible fractions could not be attributed to edge site or permanent charge adsorption or to the local coordinating environment of the adsorbed metal. Given the differences in the structure of surface-associations formed on permanent charge and edge sites of montmorillonite, and their potential effect on reversibility and bioavailability, it is important to assess both molecular structure and reversibility simultaneously. By characterizing the types of copper surface-associations formed under varying pH and background electrolyte concentrations on montmorillonite clay using X-ray absorption spectroscopy (XAS) and then assessing the kinetic reversibility of copper adsorption under similar conditions, the structural basis for reversibility trends has been explored in this study. In view of the similarities of sorption behavior of copper (this study) and other divalent metal ions such as Pb (Strawn and Sparks, 1999) and Co (Papelis and Hayes, 1996) on montmorillonite as a function of pH and background electrolyte concentration, the reversibility trends reported here may be indicative of behavior expected of other transition metal cations.

2. MATERIAL AND METHODS

2.1. Preparation of Clay

"Cheto" Ca-montmorillonite from Apache Co. Arizona was obtained from the Clay Mineral Society Repository (University of Missouri, Columbia, MO), and pretreated to remove organic and inorganic impurities using methods based on those described by Kunze and Dixon (1986). The steps in the cleaning procedure were:

1. The clay fraction (<2 μm) was separated by sedimentation of the clay suspension for a period of time that, based on Stokes Law calculations, would remove the larger sized particles (>2 μm). The supernatant clay fraction was then removed and put aside. The sedimented fraction was resuspended and the procedure was repeated until no clay particles remained in the supernatant after sedimentation. The collected supernatant from each sedimentation step was consolidated and concentrated for further treatment.
2. Free iron oxide was removed by heating 250 mL of the clay suspension in 150 mL of a sodium citrate reagent (75.3 g/L sodium citrate, 8.3 g/L $NaHCO_3$ and 70 g/L NaCl) to 75 to 80°C and adding a spatula full ($\sim$ 1 g) of dithionite-citrate-bicarbonate. After heating for an additional 15 min, the suspension was centrifuged (10000 g 10 min) and the supernatant removed. The clay was then resuspended in the sodium citrate reagent, heated for 10 min, centrifuged (10000 g 10 min) and the supernatant removed. To remove excess reagent, the clay was washed several times in 1 N NaCl.
3. Free carbonate was removed by suspension in pH=4.8 sodium acetate (136 g/L) followed by washing several times in 1N NaCl.
4. Organic matter was removed by suspension in 30% H_2O_2, heating to 80 to 85°C for 15 min followed by centrifugation (10000 g 10 min) and removal of the supernatant. This was repeated until the supernatant was colorless. To remove excess H_2O_2 the clay was then suspended in water, heated to boiling for 5 min and centrifuged to separate the clay. This procedure to remove excess H_2O_2 was repeated twice.
5. The clay was then washed in 1 N NaCl followed by repeated washing in water to removed excess NaCl. The final form of the montmorillonite was Na-montmorillonite.

2.2. Adsorption as a Function of pH and Ionic Strength

Adsorption of 50 μM copper on montmorillonite as a function of pH was measured under varying ionic strength conditions. In a 12 mL polypropylene tube, 5 mL suspension samples were prepared by combining montmorillonite (0.5 g/L) and either HNO_3 or NaOH for pH adjustment The 5 mL samples were equilibrated under atmospheric conditions at 30°C for 20 to 28 h. As metal ion adsorption reactions occur in milliseconds and very little mass transfer limitations are expected in the dilute clay suspensions used in the study, the metal was assumed to have reached equilibrium well before the end of the equilibration time. This was confirmed through experiments showing the same adsorption behavior for shorter equilibration times (several hours) as for 24 h.

After this equilibration period, the final pH (error: 0.1 (95% confidence interval or $p < 0.95$)) was then measured and the clay was separated from the solution supernatant by centrifugation (12000 g 40 min). The supernatant copper concentration was subsequently measured using an atomic absorption spectrophotometer (AAS) (error 0.005 μM ($p < 0.95$)). The amount of copper adsorbed was calculated as the difference between the copper concentration in a control sample prepared without solid and the sample supernatant concentration. Estimates of adsorption coverages of copper on edge sites were made using an edge site surface area (16 m^2/g) estimated from assumed unit cell dimensions of montmorillonite (Sposito, 1984).

2.3. X-ray Absorption Spectroscopy

Samples for XAS analysis were prepared similarly only with larger volumes to obtain enough copper-adsorbed solid for the experiment. The solids were then concentrated to a wet paste for the XAS spectroscopy. X-ray absorption spectra were collected in the fluorescence mode at the Cu K-edge at the Stanford Synchrotron Radiation Laboratory. The samples were run using either a 13 element Ge array fluorescence detector at 20K or a Lytle fluorescence detector at room temperature. No effect of temperature was found. Si (220) monochromators were used for all samples. The monochromator was detuned 50% at the highest energy of the scan to minimize contributions from higher-order harmonics. An E_o of 8979 eV was used for all of the samples. Multiple scans were collected for each sample, the number depending on the metal ion concentration, to obtain a signal-to-noise ratio sufficiently high for EXAFS analysis. The data were reduced using EXAFSPAK software (George and Pickering, 1995). For each sample the spectra collected were averaged and the background absorption was subtracted by fitting a straight line through the pre-edge region. The background subtraction in the EXAFS region was performed by fitting a three-segment spline through this region and subtracting the fit from the data in the region above the edge. The background-subtracted spectra were normalized using a Victoreen polynomial and tabulated McMaster atomic absorption fall-off coefficients. The spectra were then converted from energy to frequency space using the photoelectron wave factor, k (Brown et al., 1988; Teo, 1986). The normalized background-subtracted, k^3-weighted unsmoothed EXAFS spectra were Fourier transformed to obtain the radial structure functions (rsfs). Individual major peaks in the Fourier transform were backtransformed to produce filtered EXAFS to isolate individual shell contributions to the EXAFS. Least-squares fitting of each shell was performed to determine the coordination number (N) and bonding distance (R). The fit was further optimized by simultaneously fitting all major peaks to the unfiltered rsf. The phase and amplitude functions for Cu-O were calculated using FEFF 6.01 (Rehr and Albers, 1990) and confirmed using model compound spectra. Similarly, the phase and amplitude functions for Cu-Cu were calculated using FEFF 6.01. For the small second shell Cu-Cu peaks found in many of the Fourier transformed spectra in this study, the peak position was affected by the noise of the spectra. In particular if the k-range used in the transform included the noisier data found for the higher values (typically k=13 $Å^{-1}$ or above) or did not include enough data (k-range below approximately 11.5 $Å^{-1}$) the peak would shift resulting in approximately $\pm$ 0.03 Å variation in the fitted Cu-Cu peak. To avoid this, the k-range was kept at an intermediate value (11.5–12.5 $Å^{-1}$) and optimized to minimize the peak shift. Variability was also minimized by using similar spline fits for each sample.

To allow for meaningful comparison of the coordination numbers of the samples with small Cu-Cu peaks, several fitting parameters were allowed to float within a certain range (ΔE_o = 2–3 eV; σ^2=0.007–0.008 $Å^2$). With these constraints the peaks could be fitted well and the visual peak size correlated with the fitted coordination numbers.

2.4. Adsorption-Desorption Isotherms at Constant pH

For the purposes of this study copper adsorption was considered reversible if, over period of time equivalent to the equilibration time for adsorption, copper desorbed and reached the same equilibrium as for adsorption. To determine reversibility under this definition, adsorption and desorption isotherms were compared. For the adsorption isotherms, copper was equilibrated with montmorillonite for 24 h and the equilibrium distribution between the solution and clay was measured as described earlier. The desorption isotherm was determined by removing a portion of the total copper in the system, allowing the copper to desorb for 24 h and measuring the equilibrium distribution between the solution and clay. By measuring the desorption step over the same time period as adsorption and comparing the adsorption and desorption isotherms, a reversible reaction could be delineated from those that were either kinetically or thermodynamically limited in the desorption step and thus irreversible based on the functional definition used in this study. If the desorption isotherms coincided with the adsorption isotherm, adsorption was generally reversible. If the desorption step exhibited a steeper slope than the adsorption step, with more adsorbed at lower solution copper concentration, a portion of the adsorbed metal was not able to desorb and requilibrate in the time frame allowed and thus was considered irreversible.

Using a series of copper concentrations that ranged from 0 to 150 μM adsorption-desorption isotherms were performed at a constant pH of 4.2 and 6.8. The adsorption isotherms were prepared in the same way as described above except a range of copper concentrations was used and 5 mM PIPES buffer was added to the pH=6.8 montmorillonite samples to maintain a consistent pH over the adsorption and desorption steps. PIPES buffer has been shown to not bind metals (Yu et al., 1997) and it was found to have no effect on adsorption of copper on montmorillonite at the pH values used in the experiments. After adsorption, the pH of the samples were measured. The samples were then centrifuged (12000 g 40 min) and half of the supernatant (2.5 mL) was removed and saved for AAS measurement. For the desorption step, 2.5 mL of a copper-free solution containing the same ionic strength, buffer concentration and having the same pH was placed in the centrifuge tube. The clay was then resuspended and equilibrated for 20 to 28 h at 30°C. The pH was measured and the supernatant sampled in the same manner as the adsorption step. Using the AAS measurements (error: 0.005 μM ($p < 0.95$)) of the supernatant copper, the amount adsorbed on the solid in the adsorption and desorption steps was calculated as described above accounting for the lower total copper concentration during the desorption step.

The amount of irreversibly adsorbed copper was calculated as the difference between the amount adsorbed in the desorption step and amount adsorbed assuming the copper was fully reversible. This was done by first calculating the total amount of copper in the desorption step as the total amount added in the adsorption step minus the amount removed before desorption (i.e., half the solution phase copper during adsorption). Assuming copper adsorption is fully reversible, the desorption equilibrium would fall on the adsorption isotherm at a point that has the same total amount of copper in the system as the desorption step. This point was determined and the amount of irreversible copper was calculated as the difference between the amount on the solid under experimental conditions and the expected amount on the solid if fully reversible. In the case where experimental error was within the range of the reversible amount for a given total, it was assumed to be completely reversibly sorbed.

3. RESULTS

3.1. Adsorption as a Function of pH and Background Electrolyte Concentration

The adsorption of copper on montmorillonite as a function of pH was measured in the presence of different concentrations of background electrolyte ($NaNO_3$). Adsorption (Fig. 1) was consistent with previous research that distinguished divalent metal ion adsorption on edge and interlayer sites based on the background electrolyte concentration and pH dependence of adsorption (Fletcher and Sposito, 1989; Chen and Hayes, 1999; Papelis and Hayes, 1996; Zachara et al., 1993). Under conditions with high Na concentrations (Fig. 1: [Na]=0.1 mol/L) where the surface hydroxyl edge sites are expected to predominate, adsorption of copper on montmorillonite was pH-dependent. At lower Na concentrations (Fig. 1: [Na]=0.02 mol/L and 0 mol/L) adsorption at pH values less than 7 increased with

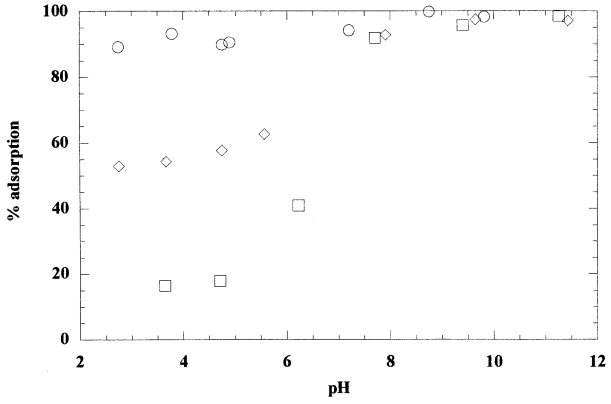

Fig. 1. Copper (50 μM) sorption on montmorillonite clay (0.5 g/L) with 0.0 M (○), 0.02 M (◇) and 0.1 M (□) added $NaNO_3$.

decreasing Na concentration. This is consistent with increased adsorption on the permanent charge sites with decreasing Na concentration. At the lowest Na concentration, pH-independent sorption was observed suggesting that copper exchange reactions on permanent charge sites was the predominant sorption process. This behavior indicates that an increase in the Na concentration resulted in a displacement of the copper from the interlayer sites and a shift in copper adsorption from the interlayer to the edge sites. This interpretation and copper adsorption are similar to that found and described previously for Co sorption as a function of pH and Na concentration (Papelis and Hayes, 1996). Based on this interpretation, Figure 2 illustrates the expected distribution of copper between the edge and interlayer sites under the pH and Na concentration conditions found in the adsorption experiments. Consistent with the data, Figure 2 shows edge site adsorption is favored with increasing Na concentration and pH, while adsorption on the interlayer is favored for low pH, low Na concentration conditions.

3.2. EXAFS Spectroscopy of Copper Surface Associations

To compare the isotherm data with the local copper coordinating environment, EXAFS spectra were collected for samples prepared under conditions comparable to the sorption experiments (Table 1). XAS analysis of such spectra provide information on the type, number and distance of the atoms within a 6 Å radius of the adsorbed copper. For the first shell of atoms surrounding the central copper atom, the interatomic distances can be estimated within an error of ± 0.01 to 0.02 Å. The coordination number can be estimated within an error of ± 10

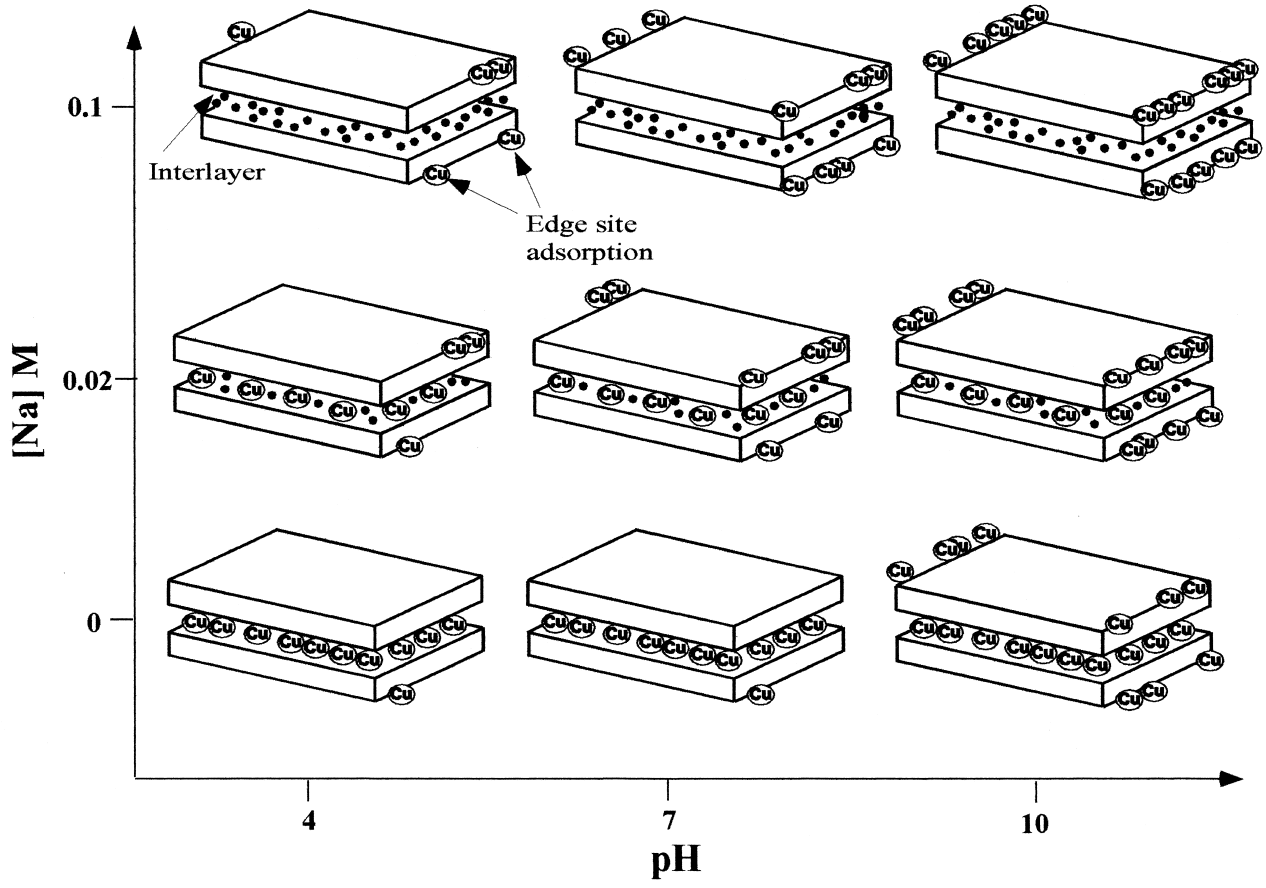

Fig. 2. Schematic diagram illustrating the effect of pH and Na concentration on the distribution of adsorbed copper on the permanent charge interlayer and edge sites of montmorillonite. The solid dots are Na atoms.

Table 1. Experimental conditions and results of EXAFS analysis.

montmorillonite concentration (g/L)	[Na+] M	pH	adsorbed Cu (μmoles/g)	predominant adsorption sites	results of EXAFS fitting: Cu-O N	Cu-O R(Å)	Cu-O σ^2(Å^2)	Cu-Cu N	Cu-Cu R(Å)	Cu-Cu σ^2(Å^2)	ΔE_o (eV)
0.5	0.00	4.0	90	permanent charge	3.9	1.97	0.0048	—	—	—	−2.8
0.5	0.00	6.0	90	permanent charge	3.7	1.97	0.0048	—	—	—	−2.3
0.5	0.00	10.0	97	permanent charge & edge	3.7	1.97	0.0047	0.9	2.98	0.0078	−2.3
0.5	0.02	4.0	53	permanent charge & edge	4.5	1.97	0.0043	0.4	2.98	0.0072	−2.3
0.5	0.02	6.8	75	permanent charge & edge	3.9	1.97	0.0047	0.4	2.98	0.0080	−2.2
0.5	0.02	7.7	90	permanent charge & edge	3.8	1.97	0.0047	0.4	2.97	0.0072	−2.4
0.5	0.10	6.2	40	edge	4.1	1.96	0.0047	0.6	2.98	0.0079	−2.7
0.5	0.10	10.0	97	edge	3.9	1.97	0.0045	1.2	2.98	0.0075	−2.6
$Cu(OH)_2$ (s)	—	—	—	—	3.5	1.98	0.0046	2.5	2.99	0.0044	−2.2
								2.7	5.80	0.0032	−2.2
$Cu(NO_3)_2$ (aq)	—	—	—	—	4.5	1.97	0.0041	—	—	—	−2.2

to 20% (O'Day et al., 1994b). The distances and coordination numbers for the second and higher shell of atoms surrounding the copper can also be determined, however, the information is less precise, depending on the number of absorber-scatterer pairs considered (Brown et al., 1988). The EXAFS spectra and radial structure functions (rsfs) for copper model compounds and copper sorbed to montmorillonite are shown in Figures 3 and 4. The peaks on rsfs correspond to the atoms neighboring the central copper with the x-axis position corresponding approximately to the interatomic distance but uncorrected for phase shift. For example, in the rsf for the $Cu(OH)_2$ (s) model compound (Fig. 3), a first shell peak was found at a distance of just under 2 Å from the central copper atom. A second shell peak is also seen at approximately 3 Å. After fitting these peaks using the procedures described in the materials and methods, the first peak was found to be consistent with a shell of Cu-O and the second peak with a second shell of Cu-Cu neighbors.

The coordination numbers and interatomic distances from the EXAFS analysis for each of the peaks as a function of solution conditions is given in Table 1. As with earlier EXAFS studies of copper, the spectra in this study (Figs. 3, 4, 5, 6 and Tables 1, 2) show a first shell coordination number ranging from 3.5 to 4.5 at 1.97 Å indicating an average of 4 oxygen atoms at this distance surrounding the central copper atom (Cheah et al., 1998; Bochatay et al., 1997). It should be noted that hydrated Cu is usually considered to be octahedrally coordinated with the two axial oxygens distorted to longer interatomic distances. In earlier studies, the axial oxygens have either not been able to be fit (Cheah et al., 1998) or only fitted after making assumptions as to the axial and equatorial interatomic distances (Korshin et al., 1998). As the method and utility of the information gained by fitting an octahedral coordination is controversial and is not significant to the main conclusions of this study, the Cu-O shell was fit using a tetrahedral coordination. For similar reasons, fitting the Cu-O first shell as a mixture of square pyrimidal and trigonal byprimidal configurations based on the results of Pasquarello et al. (2001) was deemed unwarranted.

The other feature that was found for some of the samples was a Cu-Cu peak in a second shell near 3 Å on the rsf. This indicates copper coordination in multinuclear clusters on the surfaces with the coordination number correlated to the number of copper atoms in the cluster surrounding the central copper atom.

Previous work has shown the presence of Cu-Al or Cu-Si peaks on rsfs of copper adsorbed to alumina or silica (Cheah et al., 1998). For montmorillonite, these peaks were not apparent. Evidence that the second shell peak was a Cu-Cu peak and not a Cu-Si or Cu-Al peak was provided by filtering and backtransforming this feature on the rsf. By looking at the maximum

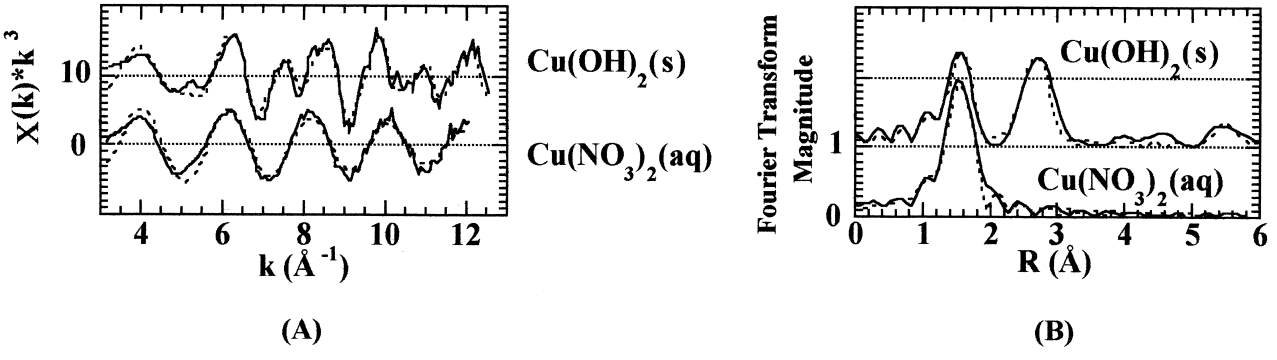

Fig. 3. EXAFS spectra (A) and radial structure functions (B) for model compounds. Dotted lines indicate fit to the data using parameters from EXAFS analysis.

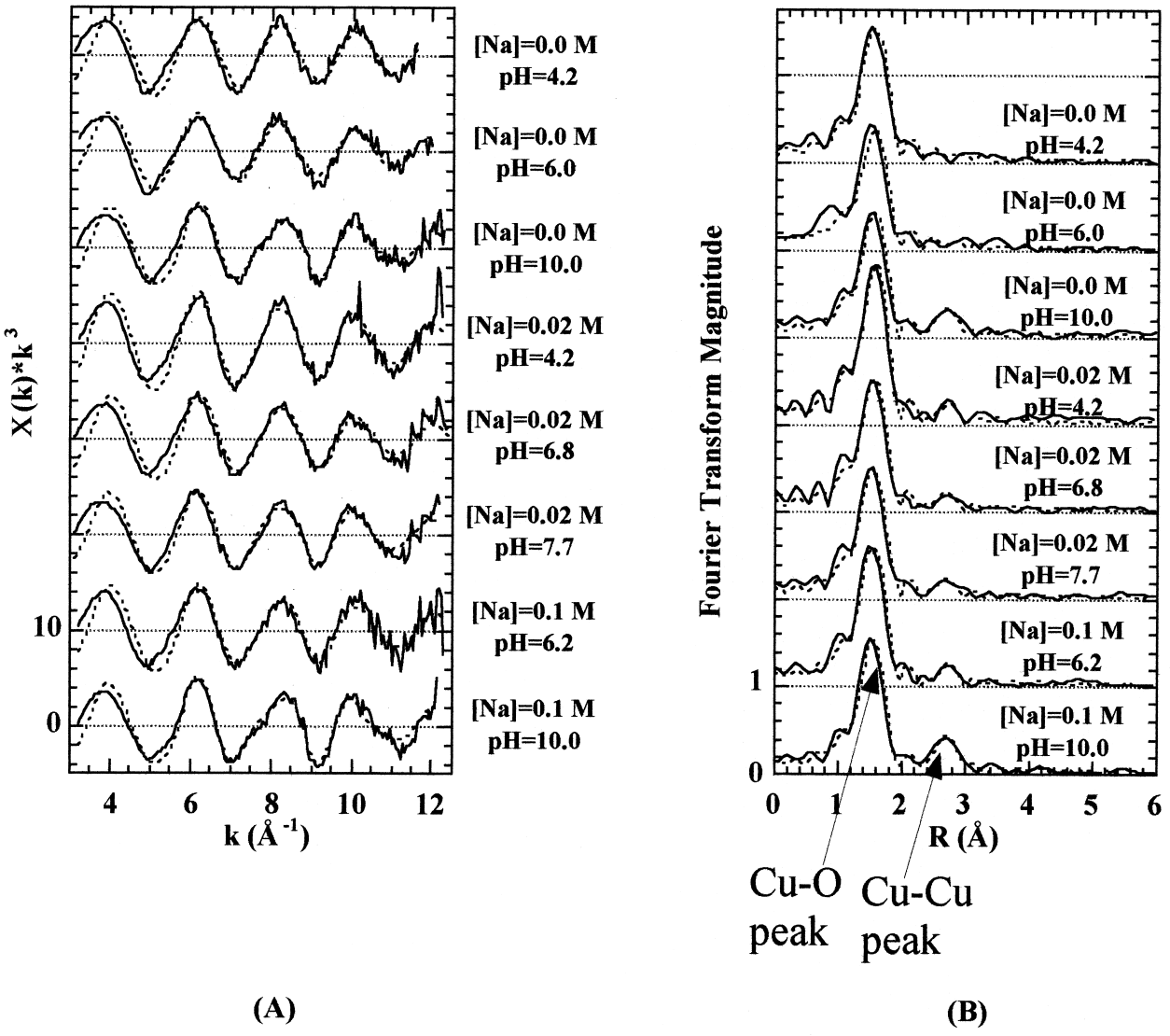

Fig. 4. EXAFS spectra (A) and radial structure functions (B) for copper adsorbed to montmorillonite under conditions described in Table 1. Dotted lines indicate fit to the data using parameters from EXAFS analysis.

amplitude envelope, it has been proposed that light backscatterers such as Si or Al can be distinguished from heavier backscatterers such as Cu (Cheah et al., 1998). For all of the spectra in this study with a second shell peak the maximum amplitude envelope ranged from 8.5 to 9.5 $Å^{-1}$. This is characteristic of a heavier element such as Cu (Cheah et al., 1998).

To interpret the structural and coordination environment of the copper clusters, data for $Cu(OH)_2$(s) were also collected. Expectations are that as clusters grow they would approach that of $Cu(OH)_2$(s) unless the surface imposes other constraints or solid-solutions form with dissolved Al ions. The Cu-Cu interatomic distances (R) of the montmorillonite samples are identical to that for $Cu(OH)_2$(s). Other studies have found a reduction of second shell metal-metal distances compared to the metal dihydroxide precipitates. For example in the study of Co on alumina (Katz and Hayes, 1995) and Co on kaolinite (O'Day et al., 1994a), second shell Co-Co distances were found to be significantly shorter compared to Co-Co distances in $Co(OH)_2$(s). Hydrotalcite-like structures, with some Al substituting for Co in the second shell, were proposed to explain the shorter Co-Co distances (O'Day et al., 1994a; Merlen et al., 1995; Bargar et al., 1997a, 1997b; Towle et al., 1997; Scheidegger et al., 1998). The possibility that Al is in the second shell was considered in this study to test if a significant improvement in the fit would result, however, no improvement was found (data not shown). It thus appears these structures are not present for copper adsorbed to montmorillonite under the conditions investigated.

The local coordinating environment of copper on montmorillonite was different depending on the type of site to which copper adsorbed. Edge site adsorption is expected to dominate at high background electrolyte concentration (see Fig. 2). Montmorillonite samples prepared under these conditions had a Cu-Cu second shell peak (Fig. 4, Table 1) with

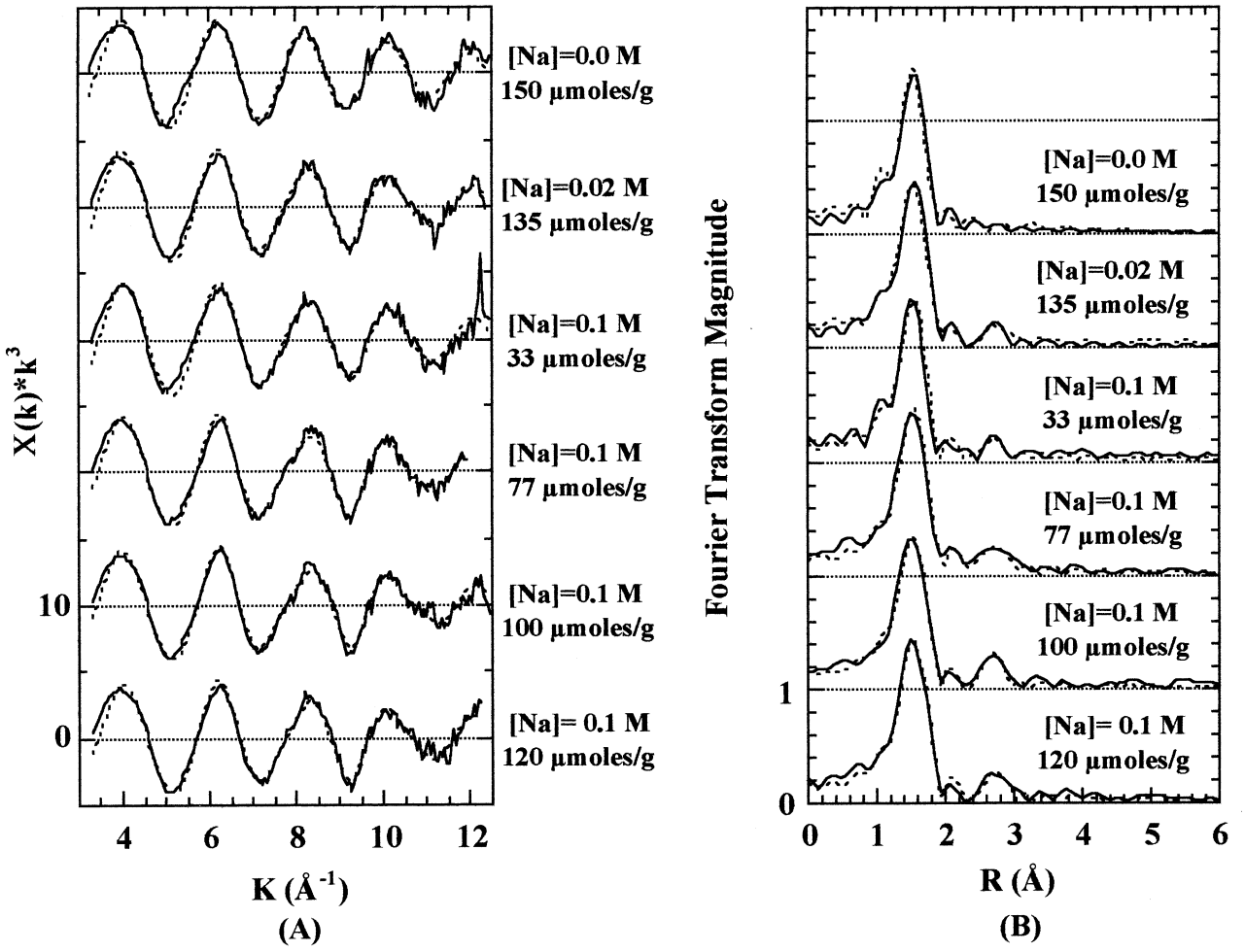

Fig. 5. EXAFS spectra (A) and radial structure functions (B) for copper adsorbed to montmorillonite at pH 6.8 (see Table 2 for details). Dotted lines indicate the fit to the data using parameters from EXAFS analysis.

Cu-Cu coordination numbers near or below 1. A coordination number of less than one has been interpreted to mean adsorption involves both monomers and dimers at these coverages (Cheah et al., 1998). The coordination numbers are less than that found for cobalt on montmorillonite where the Co-Co coordination numbers ranged between 4 and 7 (Papelis and Hayes, 1996). This may be due to the higher coverage (approximately twice as great) used in the cobalt study. In addition, this may be due to the formation of surface precipitates of cobalt under conditions where copper surface precipitates do not form.

Under low background electrolyte concentration and low pH conditions where permanent charge sites on montmorillonite are expected to predominate adsorption (see Fig. 2), the lack of a Cu-Cu peak in the rsfs is consistent with the formation of hydrated outer-sphere complexes on these sites (Fig. 4 and Table 1). This agrees with previous studies showing outer-sphere complex formation for Cu on the permanent charge layer of smectites (Brown and Kevan, 1988; McBride, 1982). It is also consistent with EXAFS spectra of Co on montmorillonite that, under similar conditions, found no second shell peak (Papelis and Hayes, 1996; Chen and Hayes, 1999).

3.3. Reversibility of Adsorption of Copper Surface-Associations on the Permanent Charge and Edge Sites of Montmorillonite

The reversibility of adsorption on montmorillonite was measured under a variety of Na concentrations and pH values to delineate the reversibility of complexes formed on the permanent charge and edge sites. As shown earlier (see Figs. 1, 2) adsorption on the permanent charge sites is favored at low pH and low Na concentrations while adsorption on the edge sites is favored at high pH and high Na concentrations. By performing adsorption-desorption measurements under these conditions (Table 3), the shifts in copper distribution between permanent charge and edge sites can be correlated with reversibility.

The reversibility of adsorption was assessed by adsorption and resuspension in a solution with half the equilibrium adsorption solution concentration. The amount of copper desorbed in the system was then measured by sampling the

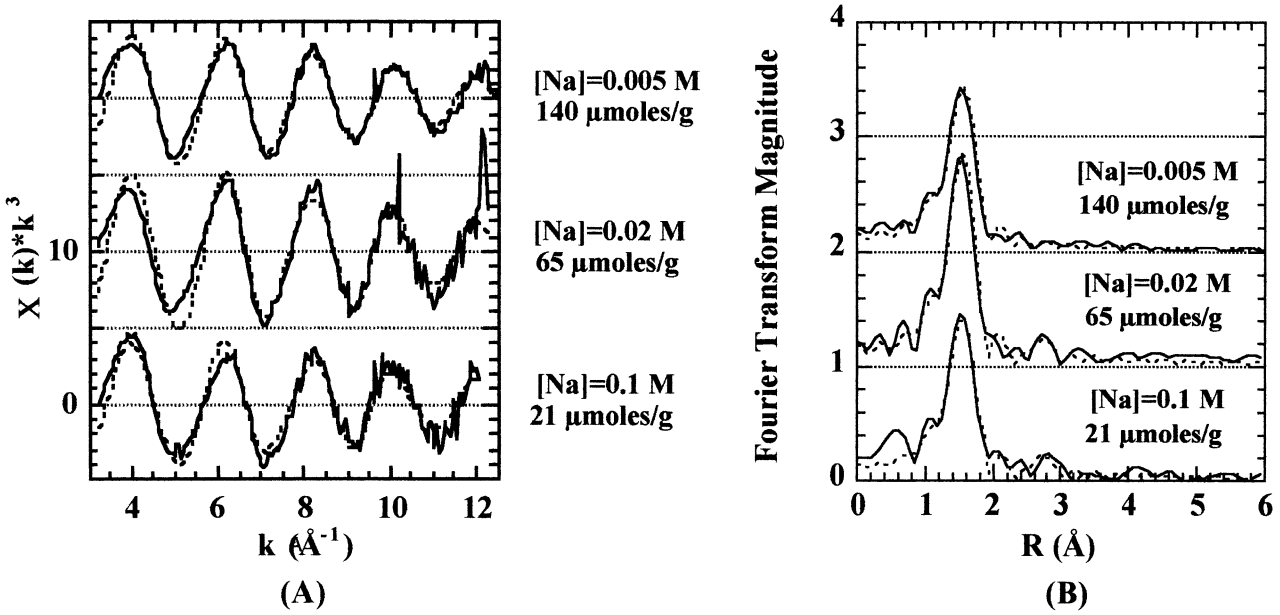

Fig. 6. EXAFS spectra (A) and radial structure functions (B) for copper adsorbed to montmorillonite at pH=4.2 (see Table 2 for details). Dotted lines indicate fit to the data using parameters from EXAFS analysis.

solution after re-equilibration. If adsorption was fully reversible the copper would be expected to requilibrate to a lower equilibrium point on the adsorption isotherm. Reversible adsorption should thus have a desorption isotherm that follows the adsorption isotherm. If at least some of the copper is irreversibly adsorbed, the desorption isotherm will exhibit a steeper slope, with more adsorbed at lower solution concentrations. By looking at the differences in the adsorption and desorption isotherms, the trends in adsorption reversibility as a function of coverage for a given pH and background electrolyte concentration (and thus distribution of copper between edge and permanent charge sites) can be determined (see Table 3).

Figure 7 shows the results of the adsorption-desorption measurements. As expected, for both pH=4.2 and 6.8 adsorption increases as the Na concentration decreases from 0.1 mol/L to near 0 mol/L. This increase in adsorption is a result of increased adsorption on the permanent charge sites and also is expected to correspond to a relative decrease in edge site adsorption. In addition, the higher concentration of reactive edge sites at pH=6.8 resulted in an increase in adsorption from pH=4.2 to 6.8 for the high background electrolyte conditions ([Na]=0.1 mol/L) where edge site adsorption predominates (Figs. 1, 2). Thus, this increase in adsorption with pH can be attributed to edge site adsorption.

For conditions where edge site adsorption is expected to predominate ([Na]=0.1 mol/L), irreversible adsorption was found at both pH=4.2 and 6.8. At pH=4.2, irreversibility occurred at low coverages (<20 μmoles/g clay; <1.25 μmoles/m^2 edge sites) and appeared to level off with more reversibility occurring at higher coverages. While edge site adsorption is favored at this Na concentration, the small number of reactive edge sites at this pH may allow adsorption to occur on permanent charge sites at higher coverages. For example, it may be the edge sites became saturated at low

Table 2. Results of EXAFS analysis of montmorillonite samples prepared under conditions comparable to adsorption-desorption experiments (Figures 3 and 4).

					results of EXAFS fitting						
					Cu-O			Cu-Cu			
[Na+] (M)	pH	adsorbed Cu (μmoles/g)	predominant adsorption sites	edge site adsorption reversibility	N	R(Å)	σ^2(Å^2)	N	R(Å)	σ^2(Å^2)	ΔE_o (eV)
0.00	6.8	150	permanent charge	—	3.6	1.97	0.0044	—	—	—	−2.9
0.02	6.8	135	permanent charge and edge	—	3.7	1.96	0.0047	0.5	2.98	0.0080	−2.5
0.10	6.8	33	edge	reversible	3.7	1.96	0.0047	0.4	2.96	0.0074	−2.0
0.10	6.8	77	edge	irreversible	3.7	1.96	0.0046	0.7	2.98	0.0075	−2.1
0.10	6.8	100	edge	irreversible	3.8	1.96	0.0052	0.8	2.97	0.0078	−2.9
0.10	6.8	120	edge	irreversible	3.6	1.96	0.0046	0.7	2.98	0.0081	−2.6
0.005	4.2	140	permanent charge	—	3.8	1.97	0.0047	—	—	—	−2.5
0.02	4.2	65	permanent charge and edge	—	4.5	1.97	0.0043	0.4	2.98	0.0072	−2.3
0.10	4.2	21	edge	irreversible	3.6	1.97	0.0048	0.5	3.00	0.0077	−2.9

Table 3. Experimental conditions for reversibility experiments.

montmorillonite concentration (g/L)	[Na+] (M)	pH	predominant adsorption sites
0.5	0.005	4.2	permanent charge
0.5	0.02	4.2	permanent charge and edge
0.5	0.10	4.2	edge
0.5	0.00	6.8	permanent charge
0.5	0.02	6.8	permanent charge and edge
0.5	0.10	6.8	edge

coverages and the reversibility observed at higher coverages is due to adsorption on the permanent charge sites. At pH=6.8 and [Na]=0.1 mol/L, a region exists where adsorption was predominantly reversible (<50 μmoles/g clay; <3.13 μmoles/m^2 edge sites) with an irreversible region at higher adsorption coverages. Under these conditions, the population of reactive edge sites is quite high and therefore the trends in adsorption-desorption at [Na]=0.1 mol/L can be attributed to the edge sites. This is evidenced by the pH dependence of adsorption at all coverages in the adsorption-desorption isotherm (e.g., changes in adsorption level at different pHs at [Na]=0.1 mol/L, Fig. 7; also see Fig. 1).

As Na concentrations decrease and adsorption on the interlayer sites increases, the trends in reversibility change. To visualize the trends more clearly, Figure 8 shows the irreversibly adsorbed copper measured in the adsorption-desorption isotherms of Figure 7 as a function of the total amount of copper adsorbed. It should be noted that the desorption experiments did not involve repeated desorption steps and thus were not designed to determine the total amount of irreversibly adsorbed copper at a given coverage. Rather they show the trends in irreversible sorption as a function of coverage. For example, the trend at [Na]=0.1 mol/L and pH=4.2 explained earlier is shown clearly (Fig. 8A) with irreversible adsorption increasing as adsorption increases at low coverages until it reaches a maximum and subsequently decreases to zero at higher coverages. Similarly, Figure 8B shows the trend at [Na]=0.1 mol/L and pH=6.8 where irreversibly adsorbed copper is near zero at low copper coverages and increases at higher coverages.

By comparing the trends for the lower Na concentrations with those at [Na]=0.1 mol/L, the reversibility of adsorption on the permanent charge sites can be assessed. If adsorption on the permanent charge sites is irreversible, the adsorption-desorption isotherms at lower Na concentrations should show increased irreversibility as indicated by a larger difference between the adsorption and desorption isotherms on Figure 7 and correspondingly higher values of irreversible copper on Figure 8. If adsorption on the permanent charge sites is reversible, the adsorption-desorption experiments should show decreased irreversibility as the copper adsorption shifts from the edge sites to the permanent charge sites. From the data it appears the permanent charge sites are reversible. Accordingly, the trend of irreversible adsorption with copper adsorption levels at pH=4.2 and [Na]=0.02 mol/L shows the same increase in irreversibly adsorbed copper and subsequent maximum found for [Na]=0.1 mol/L, however the increase is less dramatic as copper adsorption increases and the maximum occurs at a higher total adsorbed copper level. This is consistent with the expected shift in the distribution of copper from edge sites to reversible permanent charge sites. For the lowest Na concentration at pH=4.2 ([Na]=0.005 mol/L) it appears the proportion of copper on the edge sites decreases to such an extent that irreversible adsorption never reaches a maximum. A similar change in the irreversibility trends with Na concentration can be seen at pH=6.8 where the increase in irreversible adsorption found at higher coverages at [Na]=0.1 mol/L becomes less dramatic and occurs at higher total adsorbed copper levels as the Na concentration decreases (Fig. 8). This is also consistent with increasing adsorption on revers-

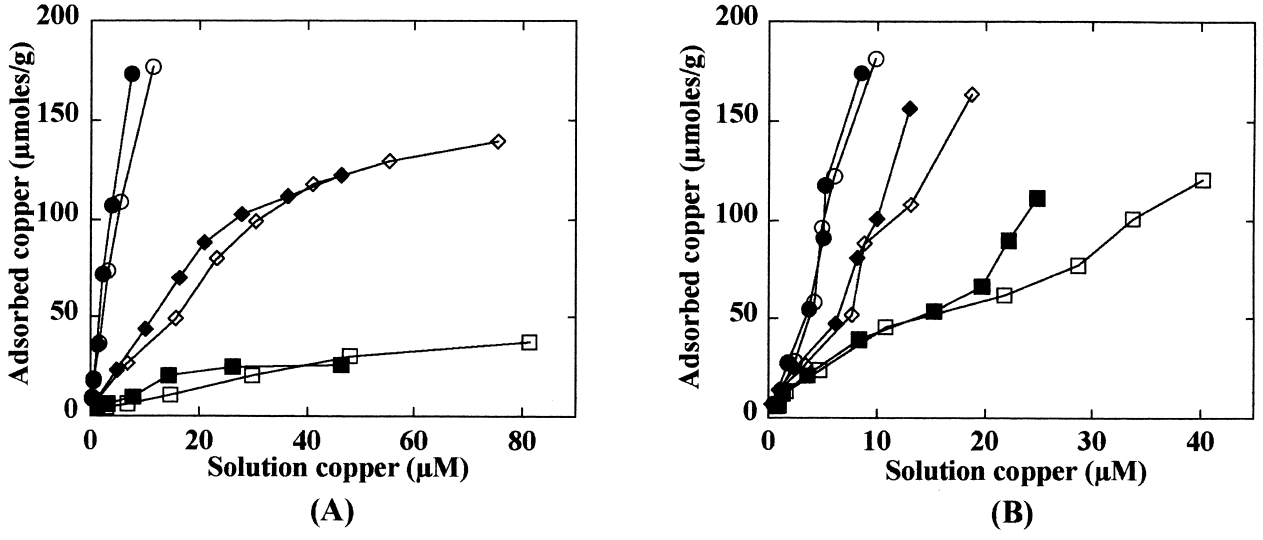

Fig. 7. Adsorption (white symbols) and desorption (dark symbols) of copper on montmorillonite (0.5 g/L) at: pH=4.2 (A) and pH=6.8 (B) with 0.005 M $NaNO_3$ (pH 4.2;○,), 0.0 M $NaNO_3$ (pH 6.8;○,), 0.02 M $NaNO_3$ (◇, ◆) and 0.1 M $NaNO_3$ (□, ■) added. The 95% confidence intervals are less than or equal to the symbol sizes shown in the plot.

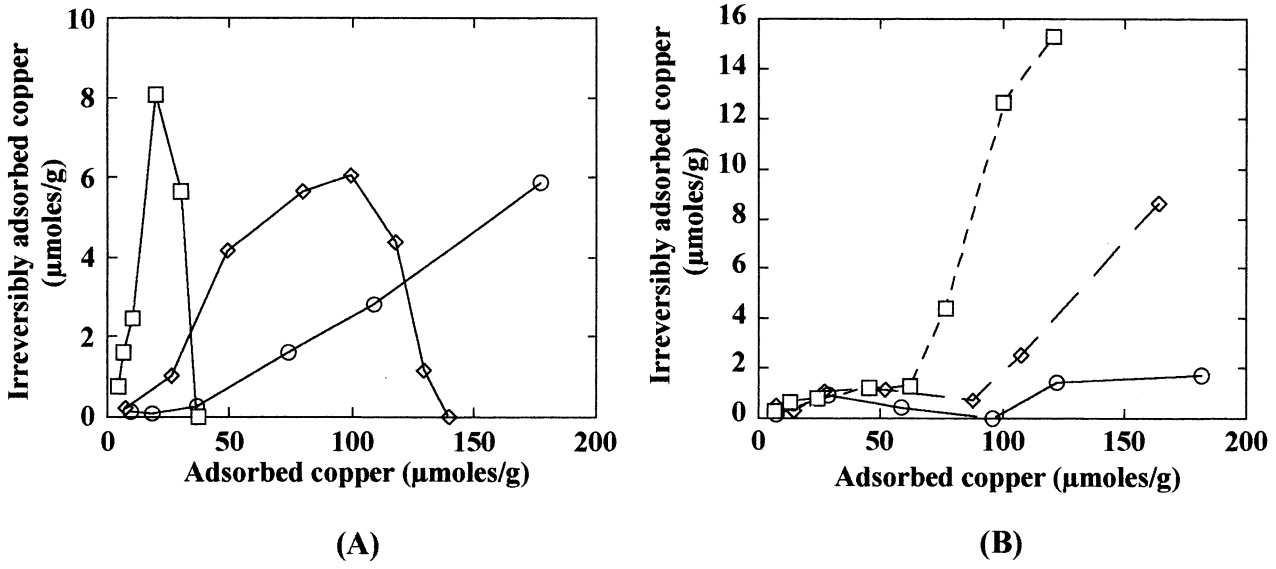

Fig. 8. Irreversibly adsorbed copper on montmorillonite calculated from the adsorption-desorption isotherms in Figure 7. pH=4.2 (A) and pH=6.8 (B). $NaNO_3$=0.1 M (□); $NaNO_3$=0.02 M (◇); $NaNO_3$=0.0 M (pH=6.8) or 0.005 M (pH=4.2)(○).

ible permanent charge sites and decreased adsorption on edge sites with decreasing Na concentration.

Thus the reversibility studies have shown that, under the conditions studied, adsorption on the permanent charge sites is reversible while adsorption on the edge sites is both reversible and irreversible depending on the pH and coverage. Irreversible adsorption on edge sites occurred at adsorption levels less than 20 μmoles/g (1.25 μmoles/m^2 edge sites) at pH=4.2 (see, e.g., position of peak irreversibility at [Na]=0.1 mol/L in Fig. 8A). At higher coverages at pH=4.2, adsorption was reversibly adsorbed to edge sites or permanent charge sites. At pH=6.8, adsorption levels less than 50 μmoles/g (3.13 μmoles/m^2) were predominantly reversible while at higher coverages adsorption was irreversible as indicated by the dramatic increase in irreversibility for [Na]=0.1 mol/L (Fig. 8B).

3.4. EXAFS Spectroscopy of Irreversibly Adsorbed Copper Surface Associations on Montmorillonite

To gain insight into the local coordinating environment of the irreversibly adsorbed copper on the edge sites of montmorillonite, EXAFS spectra were collected for samples prepared under conditions corresponding to reversible and irreversible copper adsorption observed in Figures 7 and 8. Figures 5 and 6 show the EXAFS spectra for pH=6.8 and 4.2 respectively and Table 2 shows the results of the fitting procedure. At pH=6.8 and [Na]=0.1 mol/L, where adsorption is predominantly on the edge sites (Fig. 2), spectra were collected for a low coverage sample (33 μmoles/g) where adsorption had very little irreversibility (Figs. 7, 8) and three higher coverage samples (77, 100 and 120 μmoles/g) where adsorption was found to be irreversible. All had second shell Cu-Cu peaks, with the sample where reversible adsorption is expected (33 μmoles/g) having a slightly lower coordination number (N=0.4) than the other samples (N=0.7–0.8) where irreversible adsorption was found. When less than 1, increasing coordination numbers have been interpreted to be due to an increase in the proportion of dimeric species on the surface (Cheah et al., 1998). At pH=6.8 the data is thus consistent with an increase in the ratio of dimers to monomers on the surface for the higher coverage samples where irreversible adsorption was measured.

At pH=4.2 and [Na]=0.1 mol/L at coverages (21 μmoles/g) where irreversible adsorption was observed the Cu-Cu coordination number was intermediate between the reversible and irreversible adsorption samples at pH=6.8 (N=0.5). For the [Na]=0.02 mol/L samples at pH=4.2 and 6.8, the Cu-Cu coordination numbers (N=0.4 and 0.5 respectively) were similar. As expected from the predominance of adsorption on interlayer sites under these conditions, the lowest Na concentration samples (0.005 mol/L at pH=4.2 and 0.0 mol/L at pH=6.8) displayed no second shell Cu-Cu peak and was consistent with fully hydrated copper in the interlayer.

4. DISCUSSION

4.1. Structure of Adsorbed Copper Complexes

The results of the EXAFS analysis show on the edge sites of montmorillonite, copper forms dimers or a combination of monomers and dimers at all the coverages studied. Of the possible structures of dimers outlined in the literature (Hathaway, 1987; Cheah et al., 1998) the structure that is most consistent with the Cu-O and Cu-Cu coordination numbers and interatomic distances (Table 1) is planar double bridged (Fig. 9). This structure is the basic building block of $Cu(OH)_2$(s) as evidenced by the similarity of the Cu-Cu interatomic distances of $Cu(OH)_2$(s) (2.99 Å) and the adsorbed dimers (2.98 Å). Consistent with this structure and EXAFS showing 4 coordi-

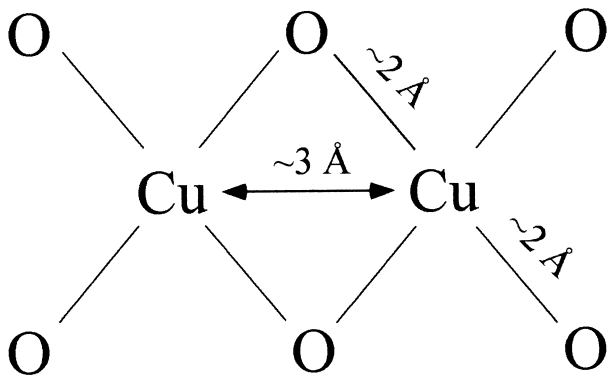

Fig. 9. Proposed planar double bridged structure of adsorbed copper dimers on montmorillonite edge sites and alumina surface hydroxyl sites. The oxygens are proposed to be from water molecules or oxygen or hydroxyl sites on the soil surface (Adapted from Hathaway, 1987).

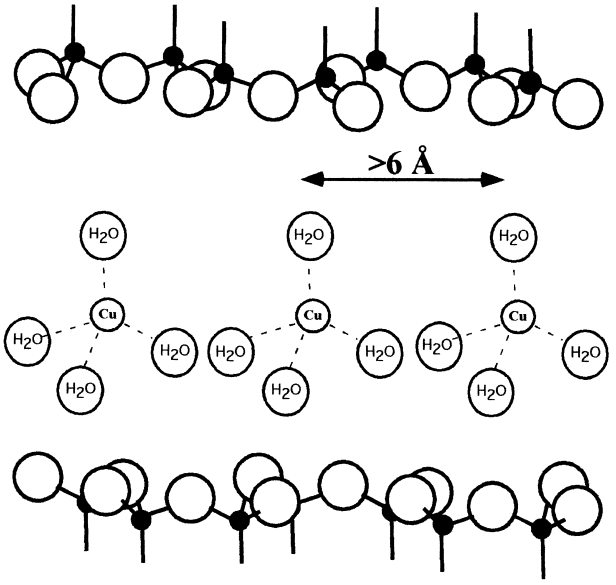

Fig. 10. Hydrated structure of copper characteristic of outer-sphere complexes formed in the interlayer of montmorillonite. The hydrated structure separates the copper atoms to beyond the range where Cu-Cu interactions can be detected using EXAFS (>6 Å).

nated oxygens around each copper, dimers on the edge sites of montmorillonite may be lying in the plane of the surface and coordinated by hydroxyl or oxygen ligands or complexed by a combination of surface sites and water molecules. The formation of dimers has been reported by others on montmorillonite edge sites using EPR (Hyun et al., 2000), and on the surface of silica using EXAFS (Cheah et al., 1998). The Cu-Cu interatomic distances for the dimers on silica were significantly shorter (2.6 Å). The lower interatomic distance indicates the dimer structure on silica differs from that on the edge sites of montmorillonite. The study by Cheah et al. (1998) proposed that the dimers on the silica surface were in a square pyramidal structure.

For copper adsorbed on the permanent charge sites of montmorillonite, EXAFS showed no second shell peak. This is consistent with the formation of an outer-sphere complex where the copper is surrounded by a shell of at least one layer of water molecules with the copper atoms far enough apart such that no Cu-Cu peak appears in the EXAFS spectra. Past spectroscopic studies of copper adsorbed to the interlayer of smectite clays (Brown and Kevan, 1988; McBride, 1982) and EXAFS studies of Co adsorbed to the permanent charge sites of montmorillonite (Papelis and Hayes, 1996; Chen and Hayes, 1999) resulted in similar conclusions for interlayer sorption. The structure is illustrated in Figure 10.

4.2. The Reversibility of Copper-Surface Associations

Based on the adsorption-desorption isotherms, copper adsorption on montmorillonite permanent charge sites is reversible. Given the hydrated structure and the weak association, evidenced by the ability of background electrolyte cations to displace interlayer metal cations, it is not surprising the outer-sphere complexes formed by copper on these sites are reversible. This is also consistent with previous studies that assessed the ideality of Me-Na exchange behavior on montmorillonite (Sposito and Mattigod, 1979; Gast, 1969, 1971; Gast et al., 1969; Sposito et al., 1981; Sposito et al., 1983a, 1983b, 1983c). These studies found ideal or near-ideal metal exchange behavoir on smectite clays. The ideal exchange behavior was attributed to adsorption on the permanent charge sites and deviations in ideality were attributed to small amounts of metal adsorbed on the edge sites (Fletcher and Sposito, 1989).

Perhaps a more interesting result is the reversibility trends found on the edge sites of montmorillonite. The adsorption-desorption isotherms indicate that copper adsorption on the edge sites is both reversible and irreversible depending on the pH and coverage. The irreversibility of adsorption has been reported for smectite clays but the origin of the irreversibility has not been addressed (McLaren et al., 1983; Wu et al., 1999). Possible explanations include the formation of kinetically irreversible multinuclear complex on the edge sites of the clay or as a result of the presence of edge sites of variable affinity, with the affinity differences among edge sites causing the variation of reversibility with coverage.

The EXAFS spectra collected under the conditions of reversible and irreversible adsorption on the clay edge sites served to test the hypothesis that multinuclear complex formation is causing the irreversibility (Table 2, Figs. 5, 6). At pH=6.8 the Cu-Cu coordination number changed from 0.4 at a coverage with reversible adsorption (33 μmoles/g) to 0.7 to 0.8 at higher coverages where irreversible adsorption was found (77–120 μmoles/g). This indicates the ratio of dimers to monomers on the surface increased for the higher coverages where irreversible adsorption was found. This data is consistent with the formation of irreversible dimers and reversible monomers on the montmorillonite edge sites. While dimers are forming at low coverages, the low coordination number indicates a large proportion of the copper is adsorbed as monomers. Lower energy and easily desorbed monomers would be expected to desorb preferentially relative to higher energy and less reversibly sorbed dimers. Monomers, in fact, could be the fraction of copper that is shown to be predominantly reversible at low coverage ($<$50 μmoles/g; pH=6.8; [Na]=0.1 mol/L; Figs. 7, 8). At higher coverages, where the population of dimers in-

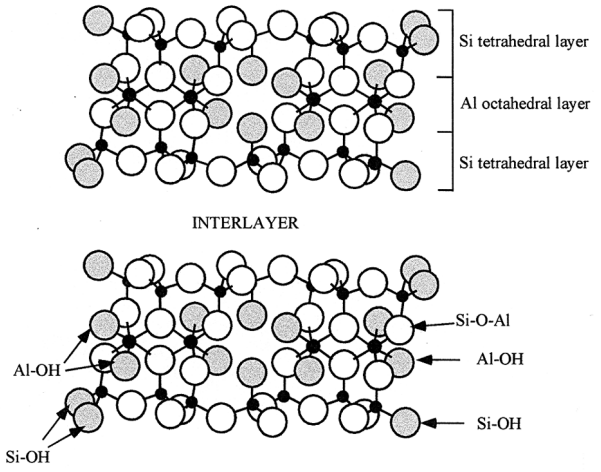

Fig. 11. The structure of montmorillonite clay showing the possible functional groups and locations of copper edge site adsorption. The shaded circles represent hydroxyl groups, the unshaded circles represent oxygen atoms and the dark circles represent the central atoms in the tetrahedral layer (Si or ismorphically substituted metals) or octahedral layer (Al or isomorphically substituted metals).

creases relative to the population of monomers, dimers likely dominate, thus causing the irreversibility shown for the higher coverages (>50 μmoles/g; pH=6.8; [Na]=0.1 mol/L; Figs. 7, 8).

For pH=4.2 at a coverage where irreversible adsorption on the edge sites was observed (21 μmoles/g; pH=4.2;; [Na]=0.1 mol/L; Figs. 7, 8) the coordination number (N=0.5) was intermediate between the reversible and irreversible coverage regions for copper samples at pH=6.8. While the coordination number does not clearly show dimer formation on the edge sites is correlated with irreversibility at pH=4.2, it is likely explanation for the observed irreversibility.

An alternative explanation for the edge site reversibility trends is the existence of different types of copper binding sites on the edges of montmorillonite. For other clays it has been speculated that adsorption on some sites is irreversible while adsorption on other sites is reversible (Clark and McBride, 1984). Figure 11 shows the structure of montmorillonite and the types of edge sites that could be involved with adsorption. Both SiOH and AlOH sites are believed to be the predominant sites for formation of metal complexes on montmorillonite clay edges while the Si-O-Al sites have been speculated to be involved in binding of metals on other clays (O'Day et al., 1994a). It may be the irreversible adsorption found at pH=4.2 results from complexes formed on a high affinity site present at this pH. The data at pH=6.8 might also be explained by adsorption to different site types, with reversible adsorption at low coverage on a pH-dependent site that is not involved in adsorption at pH=4.2 and irreversible adsorption to another site that could be similar to the aforementioned site at pH=4.2 or another site that becomes important in adsorption at higher pH. Based on energetic arguments, however, it is difficult to hypothesize sorption occurring on an irreversible site at higher coverages, assuming irreversible sorption and the energetics of complex formation are related.

Of the possible explanations of the irreversibility, the formation of dimers seems to be the most feasible explanation for the data at pH=6.8 and is a plausible explanation for the data at pH=4.2 (Figs. 7, 8). At pH=6.8 the formation of irreversible dimers that increase in number with coverage relative to reversible monomers is supported by both the EXAFS data and the energetics of adsorption. For pH=4.2, the EXAFS data are less conclusive. At this pH irreversibility may be due to dimer formation or due to formation of monomeric surface complexes on a high energy site. This conclusion is supported by recent research on desorption of Co(II) complexes from kaolinite, a clay that has only edge sites. Thompson et al. (2000) showed the fraction of copper desorbed was significantly lower for samples where multinuclear complexes (hydrotalcite precipitates) formed than for smaller adsorbates. Future research characterizing individual types of edge sites along with more reliable methods to distinguish among them will be needed to provide greater insight into this issue.

5. CONCLUSIONS

This study characterized the structure and reversibility of copper adsorbed to the permanent charge and edge sites of montmorillonite. Adsorption in the interlayer sites was consistent with outer-sphere complex formation and was reversible. For the edge sites of montmorillonite adsorption was as monomers and dimers and was irreversible at coverages less than 20 μmoles/g clay at pH=4.2 and at coverages greater than 50 μmoles/g clay at pH=6.8. At pH=6.8, Cu-Cu coordination numbers were higher for irreversible complexes on the edge sites. This is consistent with the formation of a larger proportion of irreversible dimers with increasing coverage. The coordination numbers at pH=4.2 indicates the irreversibility may be due to the formation of irreversible dimers or due to differences in the adsorption complexes formed on the various types of edge sites

In view of the fact that copper sorption behavior on montmorillonite as a function of pH and electrolyte concentration is very similar to other metals such as Pb, Cd, and Co (Strawn and Sparks, 1999; Zachara et al., 1993; Hayes and Chen, 1999; Papelis and Hayes, 1996), one might be tempted to conclude that reversibility trends reported herein might be generalized to these other metal cations, but studies to date provide conflicting evidence. In some cases, sorption irreversibility has been noted and reported to result from the formation of multinuclear species or precipitates and increasing aging time (Thompson et al., 2000; Martinez and McBride, 2000) while in other cases nearly complete reversibility is noted (Strawn et al., 1998; Strawn, 1999). More work is needed to address sorption reversibility as a function of metal ion type, coverage, pH and aging time before such generalizations, if any, can or should be made. In the broader context of predicting metal ion mobility, bioavailability, and transport in low temperature aqueous geochemical environments, improvements in geochemical models await further studies establishing the structural basis for metal ion sorption reversibility.

Acknowledgments—The authors thank two anonymous reviewers and the associate editor whose thoughtful comments helped to improve the clarity of the manuscript. We also thank the staff of the Stanford Synchrotron Radiation Laboratory (SSRL) for their help and advice in performing the XAS experiments and Dr. Chia Chen Chen for his

advice in analyzing the spectra. Support for this research was provided by the National Science Foundations Divisions of Molecular and Cellular Biosciences, Chemistry and Earth Sciences and the MPS Office of Multidisciplinary Activities through grant NSF# 9708557.

Associate editor: S. J. Traina

REFERENCES

Bargar J. R., Brown G. E. Jr, and Parks G. A. (1997a) Surface complexation of Pb (II) at oxide-water interfaces: I. XAFS and bond-valence determination of mononuclear and polynuclear Pb(II) sorption products on aluminum oxides. *Geochim. Cosmochim. Acta* **61,** 2617–2637.

Bargar J. R., Towle S. N., Brown G. E. Jr, and Parks G. A. (1966) Outer-sphere Pb(II) adsorbed at specific surface sites on single crystal α-alumina. *Geochim. Cosmochim. Acta* **60,** 3541–3547.

Bargar J. R., Brown G. E. Jr, and Parks G. A. (1997b) Surface complexation of Pb(II) at oxide-water interfaces: II. XAFS and bond valence determination of mononuclear Pb(II) sorption products and surface functional groups on iron oxides. *Geochim. Cosmochim. Acta* **61,** 2639–2652.

Bochatay L., Persson P., Lovgren L. and Brown G. E Jr. (1997) XAFS study of Cu(II) at the water-goethite (α-FeOOH) interface. *J. Phys. IV.* **7,** 819–820.

Brown D. R. and Kevan L. (1988) Aqueous coordination and location of exchangeable Cu^{2+} cations in montmorillionite clay studied by electron spin resonance and electron spin-echo modulation. *J. Am. Chem. Soc.* **110,** 743–2748.

Brown G. E. Jr, Calas G., Waychunas G. A., and Petiau J. (1988) X-ray absorption spectroscopy and its applications in mineralogy and geochemistry. In *Mineral-WaterInterface Geochemistry* (ed. F. C. Hawthorne). Vol. 18, pp. 431–512. Mineralogical Society of America, Washington, D. C.

Cheah S., Brown G. E. Jr, and Parks G. A. (1998) XAFS spectroscopy study of Cu(II) sorption on amorphous SiO_2 and γ-Al_2O_3: effect of substrate and time on sorption complexes. *J. Coll. Int. Sci.* **208,** 110–128.

Chen C. C. and Hayes K. F. (1999) X-ray absorption spectroscopy investigation of aqueous Co(II) and Sr(II) sorption at clay-water interfaces. *Geochim. Cosmochim. Acta* **63,** 3205–3215.

Clark C. J. and McBride M. B. (1984) Chemisorption of Cu (II) and Co (II) on allophane and imogolite. *Clays Clay Min.* **32,** 300–310.

Davis J. A. and Kent D. B. (1990) Surface Complexation Modeling in Aqueous Geochemistry. In *Mineral-Water Interface Geochemistry* (eds. M. F. Hochella Jr. and A. F. White), Reviews in Mineralogy, vol. 23, pp. 177-260. Mineralogical Society of America, Washington D.C.

Farquhar M. L., Charnock J. M., England K. E. R., and Vaughan D. J. (1996) Adsorption of Cu(II) on the (0001) plane of mica: a REFL-EXAFS and XPS study. *J. Coll. Int. Sci.* **177,** 561–567.

Fletcher P. and Sposito G. (1989) The chemical modelling of clay/electrolyte interactions for montmorillonite. *Clay Miner.* **24,** 375–391.

Gast R. G. (1969) Standard free energies of exchange for alkali metal cations on Wyoming bentonite. *Soil Sci. Soc. Am. Proc.* **33,** 37–41.

Gast R. G. (1971) Alkali metal cation exchange on Chambers montmorillonite. *Soil Sci. Soc. Am. Proc.* **36,** 14–19.

Gast, R. G., Van Bladel R., and Deschpande K. B. (1969) Standard heats and entropies of exchange for alkali metals on Wyoming bentonite. *Soil Sci. Soc. Am. Proc.* **33,** 661–664.

George G. N. and Pickering I. J. (1995) EXAFSPAK-A suite of computer programs for analysis of X-ray absorption spectra, Stanford Synchrotron Radiation Laboratory, Palo Alto, CA.

Hathaway B. J. (1987) In *Comprehensive coordination chemistry- the synthesis, reactions, properties and application of coordination compounds* (eds. G. Wilkinson, R. D. Gillard and J. A. McCleverty), pp 533. Pergamon, Oxford.

Hayes K. F. and Katz L. E. (1995) Application of x-ray absorption spectroscopy for surface complexation modeling of metal ion sorption. In *Physics and Chemistry of Mineral Surfaces* (eds. P. V. Brady), pp 147-224. CRC Press, New York.

Hayes K. F. and Traina S. J. (1998) Metal Ion Speciation and Its Significance in Ecosystem Health. In *Soil Chemistry and Ecosystem Health* (eds P. M. Huang), SSSA Special Publication Number 52, pp 45-84. Soil Science Society of America, Inc., Madison, WI.

Hudson E. A., Terminello L. J., Viani B. E., Denecke M., Reich T., Allen P. G., Bucher J. J., Shuh D. K., and N. M. Edelstein. (1999) The structure of U^{+6} sorption complexes on vermiculite and hydrobiotite. *Clays Clay Miner.* **47,** 439–457.

Hyun S. P., Cho Y. H., Kim S. J., and Hahn P. S. (2000) Cu (II) sorption mechanism on montmorillonite: an electron paramagnetic resonance study. *J. Coll. Int. Sci.* **222,** 254–261.

Korshin G. V., Frenkel A. I., and Stern E. A. (1998) EXAFS study of the inner shell structure in copper (II) complexes with humic substances. *Env. Sci. Tech.* **32,** 2699–2705.

Kunze G. W. and Dixon J. B. (1986) Pretreatment for mineralogical analysis. In *Methods of soil analysis, part 1. physical and mineralogical methods* (ed. A. Klute), pp 91–100. American Society of Agronomy-Soil Science Society of America, Madison.

Martinez C. E. and McBride M. B. (2000). Aging of coprecipitated Cu in Alumina. Changes in the structural location, chemical form, and solubility. *Geochim. Cosmochim. Acta* **64,** 1729–1737.

McBride M. B. (1982) Hydrolysis and dehydration reactions of exchangable Cu^{2+} on hectorite. *Clays Clay Min.* **30,** 200–206.

McBride M. B. (1994) Environmental Soil Chemistry. Oxford University Press, New York.

McLaren R. G, Williams J. G. and Swift R. S. (1983) Some observations on the desorption and distribution behavior of copper with soil components. *J. Soil Sci.* **34,** 325–331.

Merlen E., Gueroult P., de la Caillerie J.-B. d. E., Rebours B., Bobin C., and Clause O. (1995) Hydrotalcite formation at the alumina/water interface during impregnation with Ni (II) aqueous solutions at neutral pH. *Appl. Clay Sci.* **10,** 45–56.

O'Day P. A., Parks G. A.and Brown G. E. (1994a) Molecular structure and binding sites of cobalt (II) surface complexes on kaolinite from x-ray abosorption spectroscopy. *Clays Clay Min.* **3,** 337–355.

O'Day P. A., Brown G. E. and Parks G. A. (1994b) X-ray absorption spectroscopy of cobalt (II) multinuclear surface complexes and surface precipitates on kaolinite. *J. Coll. Int. Sci.* **165,** 269–289.

Papelis L. P. and Hayes K. F. (1996) Distinguishing between interlayer and external sorption site of clay minerals using x-ray absorption spectroscopy. *Coll. Surf.* **107,** 89–96.

Pasquarello A., Petri I, Salmon P. S., Parisel O., Car R., Toth E., Powell D. H., Fischer H. E., Helm L., and Merbach A. E. (2001). First solvation shell of the Cu(II) aqua ion: evidence for fivefold coordination. *Science.* **291,** 856–859.

Rehr J. J. and Albers R. C. (1990) Scattering-matrix formulation for curved-wave multiple scattering theory: Application to x-ray absorption fine structure. *Phys. Rev.* **B41,** 8139–8149.

Scheidegger, A. M., Strawn, D. G., Lamble, G. M., and Sparks, D.L. (1998) The kinetics of mixed Ni-Al hydroxide formation in clays and Al oxide minerals: a time-resolved XAFS study. *Geochim. Cosmochim. Acta* **62,** 2233–2245.

Schlegel M. L., Manceau A., Chateigner D., and Charlet L. (1999) Sorption of metal ions on clay minerals. 1. Polarized EXAFS evidence for the adsorption of Co on the edges of hectorite particles. *J. Coll. Int. Sci.* **215,** 140–158.

Sposito G. (1984) The Surface Chemistry of Soils. Oxford University Press, New York.

Sposito G., Holtzclaw K. M., Charlet L., Jouany C., and Page A. L. (1983a) Cation selectivity in sodium-calcium and sodium-magnisium exchange in Wyoming bentonite at 298 K. *Soil Sci. Soc. Am. J.* **47,** 917–921.

Sposito G., Holtzclaw K. M., Charlet L., Jouany C., and Page A. L. (1983b) Sodium-calcium and sodium-magnesium exchange in Wyoming bentonite in perchlorate and chloride background ionic media. *Soil Sci. Soc. Am. J.* **47,** 51–56.

Sposito G., Jouany C., Holtzclaw K. M., and LeVesque X. (1983c) Calcium-magnesium exchange in the presence of adsorbed sodium. *Soil Sci. Soc. Am. J.* **47,** 1081–1085.

Sposito G., Holtzclaw K. M., Johnston C. T., and LeVesque X. (1981) Thermodynamics of sodium-copper exchange on Wyoming bentonite at 298 K. *Soil Sci. Soc. Am. J.* **45,** 1079–1084.

Sposito G. and Mattigod S.V. (1979) Ideal behavior in Na-trace metal

cation exchange on Camp Berteau montmorillonite. *Clays Clay Min.* **27,** 125–128.

Strawn D. G. (1999) Kinetics and mechanisms of Pb(II) sorption and desorption in soils and soil minerals. Ph.D. Dissertation. University of Delaware.

Strawn D. G., Scheidegger A. M., and Sparks D. L. (1998) Kinetics and mechanisms of Pb(II) sorption and desorption at the aluminum oxide-water interface. *Env. Sci Tech.* **32,** 2596–2601.

Strawn D. G. and Sparks D. L. (1999) The use of XAFS to distinguish between inner- and outer-sphere lead adsorption complexes on montmorillonite. *J. Coll. Int. Sci.* **216,** 257–269.

Teo, B. K. (1986) EXAFS: Basic Principles and Data Analysis, Springer-Verlag, Berlin.

Thompson H. A., Parks G. A., and Brown G. E. Jr. (2000). Formation and release of cobalt(II) and precipitation products in aging kaolinite-water slurries. *J. Coll. Int. Sci.* **222,** 241–253.

Towle S. N., Bargar J. R., G. E. Brown Jr. and Parks G. A. (1997) Surface precipitation of Co (II) (aq) on Al_2O_3. *J. Coll. Int. Sci.* **187,** 62–82.

Wu J., Laird D. A., and Thompson M. L. (1999) Sorption and desorption of copper on soil clay components. *J. Env. Qual.* **28,** 334–338.

Yu Q., Kandegedara A., Xu Y. and Rorabacher, D. B. (1997) Avoiding interferences from Good's Buffers: a contiguous series of noncomplexing tertiary amine buffers covering the entire range of pH=3–11. *Anal. Biochem.* **253,** 50–56.

Zachara J. M., Smith S., McKinley J. P., and Resch J. T. (1993) Cadmium sorption on specimen and soil smectites in sodium and calcium electrolytes. *Soil Sci. Soc. Am. J.* **57,** 1491–1505.